The American Journal of Pathology, Vol. 193, No. 2, February 2023

The American Journal of PATHOLOGY
ajp.amjpathol.org

See related Commentary on page 136

MOLECULAR PATHOGENESIS OF GENETIC AND INHERITED DISEASES

Identification of an Electrogenic $2Cl^-/H^+$ Exchanger, ClC5, as a Chloride-Secreting Transporter Candidate in Kidney Cyst Epithelium in Tuberous Sclerosis

Sharon Barone,*† Marybeth Brooks,*† Kamyar Zahedi,*† L. Shannon Holliday,‡ John Bissler,§¶ Jane J. Yu,‖ and Manoocher Soleimani*†

From Research Services, Veterans Health Care Medical Center, Albuquerque, New Mexico; the Department of Medicine,† University of New Mexico Health Sciences Center, Albuquerque, New Mexico; the Department of Orthodontics,‡ University of Florida, Gainesville, Florida; the Department of Pediatrics,§ University of Tennessee Health Science Center and Le Bonheur Children's Hospital, Memphis, Tennessee; the Department of Pediatrics,¶ St. Jude Children's Research Hospital, Memphis, Tennessee; and the Department of Internal Medicine,‖ University of Cincinnati College of Medicine, Cincinnati, Ohio*

Accepted for publication October 11, 2022.

Address correspondence to Manoocher Soleimani, M.D., Department of Medicine, University of New Mexico School of Medicine, 915 Camino de Salud, IDTC Rm. 3315, Albuquerque, NM 87131. E-mail: msoleimani@salud.unm.edu.

Kidney cyst expansion in tuberous sclerosis complex (TSC) or polycystic kidney disease (PKD) requires active secretion of chloride (Cl^-) into the cyst lumen. In PKD, Cl^- secretion is primarily mediated via the cystic fibrosis transmembrane conductance regulator (CFTR) in principal cells. Kidney cystogenesis in TSC is predominantly composed of type A intercalated cells, which do not exhibit noticeable expression of CFTR. The identity of the Cl^--secreting molecule(s) in TSC cyst epithelia remains speculative. RNA-sequencing analysis results were used to examine the expression of FOXi1, the chief regulator of acid base transporters in intercalated cells, along with localization of Cl^- channel 5 (ClC5), in various models of TSC. Results from *Tsc2*$^{+/-}$ mice showed that the expansion of kidney cysts corresponded to the induction of Foxi1 and correlated with the appearance of ClC5 and H^+-ATPase on the apical membrane of cyst epithelia. In various mouse models of TSC, *Foxi1* was robustly induced in the kidney, and ClC5 and H^+-ATPase were expressed on the apical membrane of cyst epithelia. Expression of ClC5 was also detected on the apical membrane of cyst epithelia in humans with TSC but was absent in humans with autosomal dominant PKD or in a mouse model of PKD. These results indicate that ClC5 is expressed on the apical membrane of cyst epithelia and is a likely candidate mediating Cl^- secretion into the kidney cyst lumen in TSC. *(Am J Pathol 2023, 193: 191–200; https://doi.org/10.1016/j.ajpath.2022.10.007)*

Tuberous sclerosis complex (TSC), an autosomal dominant disorder that affects >1 million people worldwide, is caused by the lack of functional TSC1 (hamartin) or TSC2 (tuberin) proteins.[1–6] TSC1 is a co-chaperone that regulates the stability of TSC2, while the latter negatively regulates the activation of the mammalian target of rapamycin (mTOR) through modifying the GTPase activity of RHEB.[7,8] Inactivating mutations in TSC genes lead to unregulated activity of mTOR, a serine threonine kinase that regulates cell

Supported by a VA Merit Review Award (2I01BX001000-10); a Dialysis Clinic Inc. grant (DCI C-4149); and NIH/NHLBI grant T32 HL007736 (Minority Institutional Research Training Program; T.C. Resta, Principal Investigator, and M.S., Mentor). This research made use of the Fluorescence Microscopy and Cell Imaging Shared Resource, which is supported in part by the University of New Mexico Comprehensive Cancer Center Support Grant NCI P30CA118100, and the Department of Pharmaceutical Sciences, College of Pharmacy preclinical imaging core. M.S. is a Senior Clinician Scientist Investigator with the Veterans Health Administration.

Disclosures: None declared.

https://doi.org/10.1016/j.ajpath.2022.10.007

proliferation in response to environmental conditions (eg, availability of nutrients).[5,9–13] TSC affects multiple organs, including the kidney, lung, and brain. In the kidney, TSC is associated with the development of benign tumors (angiomyolipomata) and cysts, which result in renal parenchyma damage and eventually renal failure.[14–17]

Despite extensive studies examining the initiating events in TSC, little is known about the factors that promote cyst expansion, especially considering that the epithelial cells lining the cysts are predominantly composed of type A intercalated (A-intercalated) cells.[18,19] Multiple genetically engineered TSC mouse models were used to show that cyst enlargement was associated with the gradual disappearance of principal cells and hyperproliferation of A-intercalated cells. Examination of the cystic epithelium of patients with TSC also revealed the predominance of A-intercalated cells and a paucity of principal cells.[18] Recent studies indicate that the disruption of Notch signaling between principal and intercalated cells, and the consequent activation of FOXI1 and deactivation of HES1 transcription factors, may play critical roles in kidney cyst formation.[19]

The crucial step in the expansion of kidney cysts entails the secretion of fluid into the cyst lumen, which is dependent on chloride (Cl^-) secretion from the cyst epithelium into the cyst lumen. In autosomal dominant polycystic kidney disease (ADPKD), the main mechanism mediating Cl^- secretion into cysts is via the cystic fibrosis transmembrane conductance regulator (CFTR) in principal cells that is activated consequent to cAMP/protein kinase A stimulation by arginine vasopressin.[20] It is highly unlikely that CFTR is playing a major role in Cl^- secretion into the kidney cysts in TSC. The main reason for this assertion is a profound reduction in the number of CFTR-containing principal cells in cyst epithelia in patients with TSC.[19] As such, apical Cl^- transporters in A-intercalated cells may play crucial roles in this regard. However, little information is available on such molecules in A-intercalated cells.

RNA-sequencing analysis in the kidneys of *Tsc1* knockout (KO) (*Tsc1/Aqp2* Cre) mice revealed a significant enhancement in the expression of Cl^- channel 5 (ClC5). Immunofluorescence studies showed the apical localization of ClC5 in A-intercalated cells in the cyst epithelia in *Tsc1* KO mice.[19] Additional studies further revealed the co-localization of ClC5 and H^+-ATPase on the apical membrane of cyst epithelia in *Tsc1* KO mice.[19] ClC5, a $2Cl^-/H^+$ exchanger, is located in the endosomal membrane in proximal tubule and A-intercalated cells of the collecting duct, where it plays a critical role in dissipating H^+ secretion and membrane depolarization by H^+-ATPase.[21–24] Whether ClC5 expression on the apical membrane of cyst epithelia is widespread and involves both human and mouse models of TSC or is only unique to mice with principal cell–specific deletion of *Tsc1* remains speculative.

RNA-sequencing studies further showed the induction of *Foxi1* in kidneys of *Tsc1* KO mice. *Foxi1* is critical to the proliferation and growth of intercalated cells and is a main regulator of their H^+-ATPase subunits.[25,26] The additional deletion of *Foxi1* in *Tsc1* KO mice abrogated the kidney cystogenesis in *Tsc1* KO mice.[19] Whether *Foxi1* induction correlates with the expansion of kidney cysts in TSC remains unknown.

In the present studies, kidneys from mice with global, as well as principal cell–specific or pericyte-specific, inactivation of *Tsc1* or *Tsc2* were investigated. The expression of *Foxi1*, along with the localization of H^+-ATPase and ClC5, was studied in cyst epithelia. The results show the unique localization of ClC5 on the apical membrane of cyst epithelium in both human and mouse models of TSC.

Materials and Methods

Tsc2 Heterozygote Mice

The homozygous *Tsc2* KO mice ($Tsc2^{-/-}$) are embryonically lethal, whereas *Tsc2* heterozygote ($Tsc2^{+/-}$) mice are viable and develop many characteristics of Tsc2 disease, including multiple bilateral renal cystadenomas by 15 months of age.[15] Three oligonucleotides were used for PCR genotyping in these animals: H162 (5′-CAAACCCACCTCCTCAAGCTTC-3′); H163 (5′-ATTGCGGCCTCAACAATCG-3′); and H164 (5′-AGACTGCCTTGGGAAAAGCG-3′). The following conditions were used for the PCR genotyping: 94°C for 2 minutes, 1 cycle; 94°C for 30 seconds, 58°C for 30 seconds, and 72°C for 1 minute, 35 cycles; 72°C for 5 minutes, 1 cycle; and hold 4°C producing an 86 bp wild-type (WT) band and a 105 bp mutant band.

Generation of Principal Cell–Specific Knockout of Tsc1 or Tsc2 Mice or Pericyte-Specific Tsc1 KO Mice

The details regarding the generation of principal cell–specific *Tsc1* KO (*Tsc1/Aqp2* cre) or *Tsc2* KO (*Tsc2/Aqp2* cre) mice and pericyte-specific *Tsc1* KO mice (*Tsc1/renin* cre) have been previously reported from our laboratories.[18,19] To generate *Tsc1* or *Tsc2* KO mice, floxed mice for *Tsc1* (#005680; The Jackson Laboratory, Bar Harbor, ME)[27,28] or *Tsc2* (#027458; The Jackson Laboratory)[29] were crossed with *Aqp2*-cre mice (#006881; The Jackson Laboratory)[30,31] to generate principal cell–specific *Tsc1* or *Tsc2* KO mice. The following primer sequences were used to verify the presence or absence of *Aqp-2* cre transgene: mAqp-2 F (5′-CCTCTGCAGGAACTGGTGCTGG-3′) and CreTag R (5′-GCGAACATCTTCAGGTTCTGCGG-3′). To generate pericyte-specific deletion of *Tsc1*, floxed *Tsc1* mice were crossed with renin cre mice.[18,32]

Kidney Section from TSC and Patients with ADPKD

Kidney sections from patients with TSC were obtained with institutional review board approval and de-identified before processing for immunofluorescence studies. Slides with kidney sections from patients with ADPKD were acquired

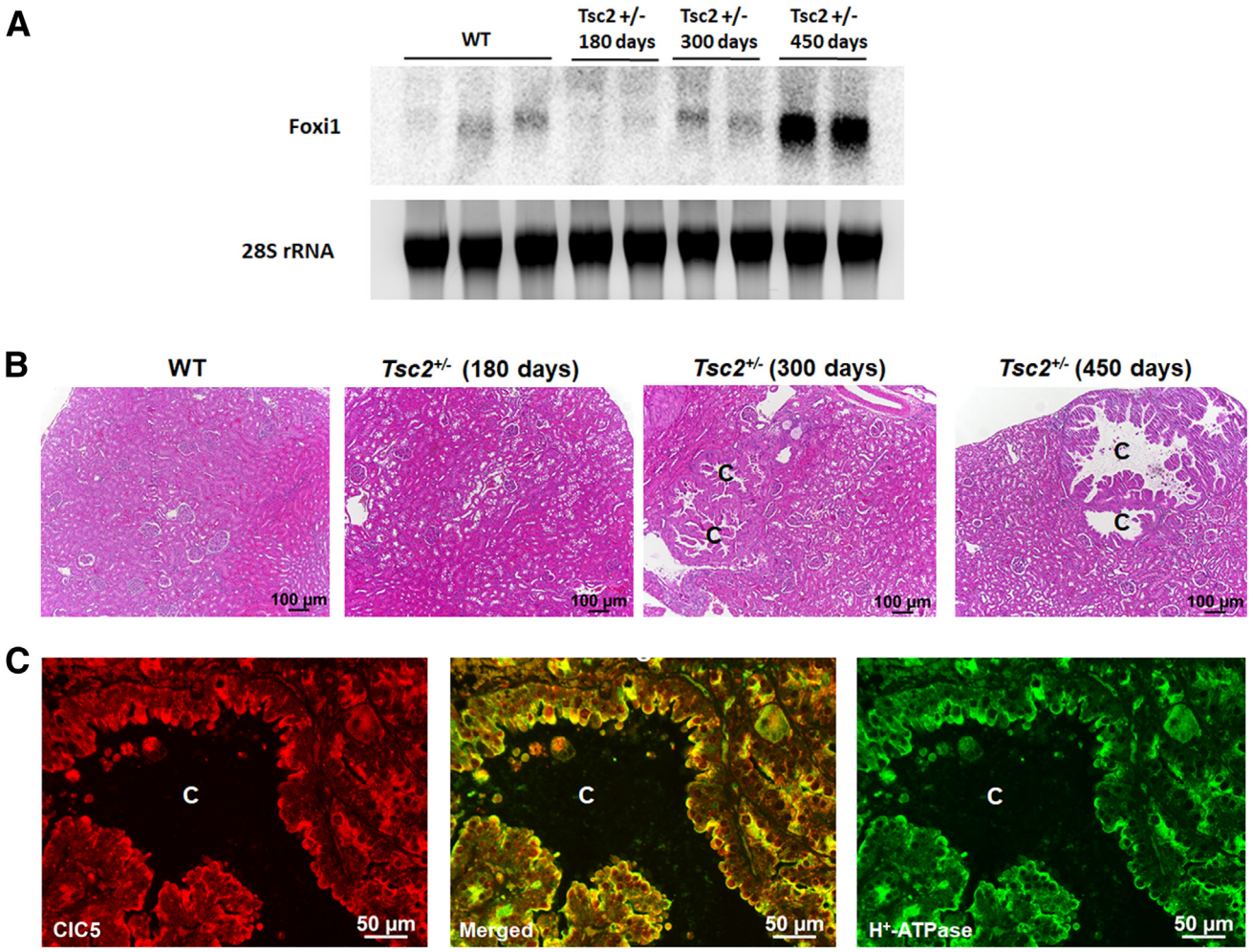

Figure 1 Examination of *Foxi1* expression and chloride channel 5 (ClC5) localization in kidneys of wild-type (WT) and $Tsc2^{+/-}$ mice. **A:** Ontogeny of *Foxi1* expression in kidneys of $Tsc2^{+/-}$. *Foxi1* expression in the kidney is low in WT and 180- or 300-day—old mice but is significantly upregulated at 450 days. **B:** Histologic analysis of kidneys of WT and $Tsc2^{+/-}$ mice. Hematoxylin and eosin of WT and 180-, 300-, and 450-day—old $Tsc2^{+/-}$ mice. No cysts are visible at 180 days; however, there are small cysts present at 300 days and large mature cysts detected at 450 days. **C:** Double immunofluorescence labeling of ClC5 and H^+-ATPase antibodies in kidneys of $Tsc2^{+/-}$ mice. ClC5 (**left panel**) and H^+-ATPase (**right panel**) with the merged image (**middle panel**). Global *Tsc2* KO mice are lethal. Scale bars: 100 μm (**B**); 50 μm (**C**). Original magnification: ×10 (**B**); ×40 (**C**). "C" represents cysts.

from the Biospecimen Repository of the Baltimore Polycystic Kidney Disease (PKD) Research and Clinical Core Center (Baltimore, MD).

Histologic Analysis of Kidney Sections

Mouse kidneys were stained with hematoxylin and eosin (H&E) and visualized under a Zeiss Axioskop 2 MOT microscope fitted with an AxioCam HR color camera (Carl Zeiss AG, Oberkochen, Germany). Images were obtained by using AxioVision Image Acquisition Software (Carl Zeiss AG).

Northern Blot Analysis

After harvesting the kidneys from WT and *Tsc* KO mice, total kidney RNA was isolated by using the TRI Reagent (Molecular Research Center, Cincinnati, OH) protocol. A UV-1600PC spectrophotometer (VWR, Radnor, PA) was used to measure RNA concentrations. The extracted RNA was size fractionated by agarose gel electrophoresis under denaturing conditions and transferred to a nitrocellulose membrane. The Foxi1 cDNA probe used for Northern blot hybridizations was generated by RT-PCR using the following gene-specific DNA oligonucleotides: 5′-AGCAAGGCTGGCTGGCAGAA-3′ and 5′-TGGCCACGGAGCGGCTAATA-3′. Hybridization with a radioactive ^{32}P labeled Foxi1 cDNA probe was performed according to published protocols.[18,33,34]

Immunofluorescence Microscopy

Mouse kidneys were harvested and placed in 4% paraformaldehyde at 4°C for 24 hours and transferred to 70% ethanol for storage at 4°C. Fixed tissues were paraffin embedded and then cut in 5-μm sections. To prepare for immunofluorescence staining, slides were baked at 60°C for

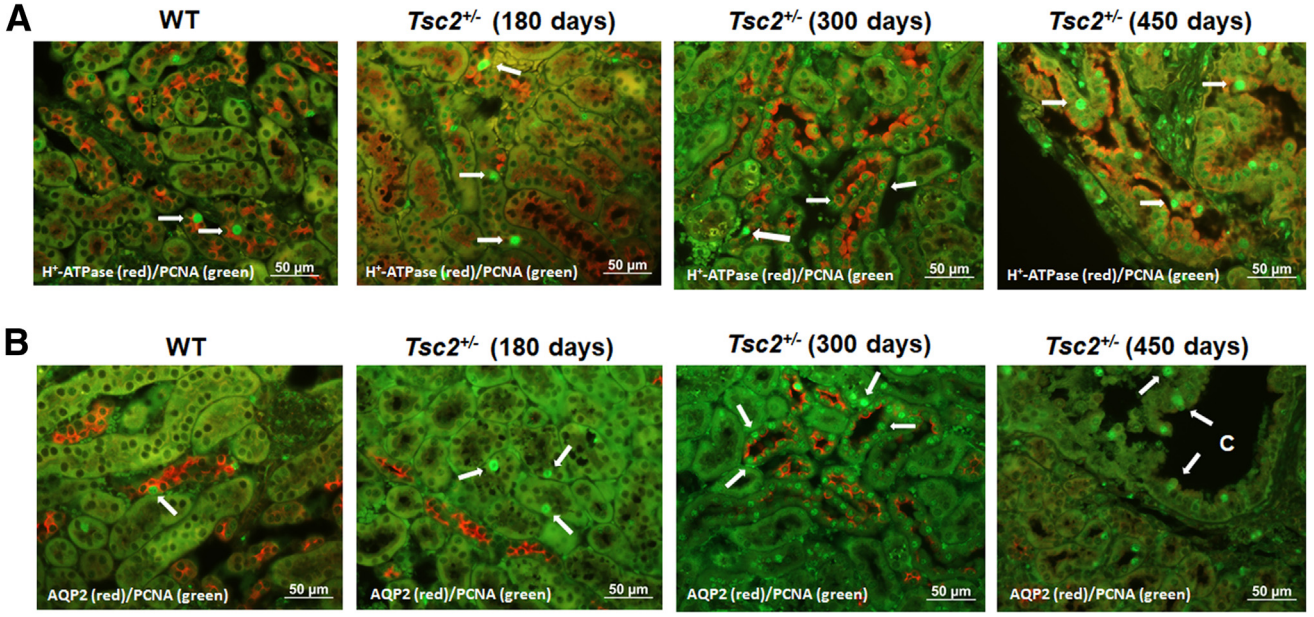

Figure 2 Cyst epithelium proliferation in kidneys of $Tsc2^{+/-}$ mice. **A:** Double immunofluorescence merged images of H^+-ATPase (red) and proliferating cell nuclear antigen (PCNA) (green) in wild-type (WT) and 180-, 300-, and 450-day–old $Tsc2^{+/-}$ mice. Note the increasing number of PCNA-positive cells at days 300 and 450. **B:** Double label immunofluorescence merged images with AQP2 (red) and PCNA (green). Although there is an age-related increase in PCNA-positive cells (day 300), there is a lack of AQP2-positive staining due to the paucity of principal cells in the cyst epithelium in $Tsc2^{+/-}$ mice. **White arrows** point to PCNA-positive cells. Scale bars = 50 μm. Original magnification, ×40. "C" represents cysts.

2 hours and allowed to cool to room temperature for 30 minutes. After deparaffinization in xylene followed by rehydration in decreasing concentrations of ethanol, slides underwent antigen retrieval and were incubated with antibodies against ClC5 (MilliporeSigma, St. Louis, MO)[21] and either H^+-ATPase B1/B2 subunit (Santa Cruz Biotechnology, Dallas, TX), H^+-ATPase E subunit, or AQP2 (a kind gift from Dr. Anne Blanchard)[35] overnight in a humidity chamber at 4°C. To examine cell proliferation in $Tsc2^{+/-}$ mice, slides were incubated in proliferating cell nuclear antigen along with either polyclonal H^+-ATPase (generated in our laboratory) or AQP2 (Santa Cruz Biotechnology). The following day, slides were washed in phosphate-buffered saline and incubated in Alexa Fluor 594 goat anti-rabbit IgG, as well as Alexa Fluor 488 goat anti-mouse IgG secondary antibodies (Thermo Fisher Scientific, Waltham, MA) for 2 hours at room temperature. After washing in phosphate-buffered saline and allowing slides to dry, they were cover-slipped using VECTASHIELD HardSet mounting media (Vector Laboratories, Newark, CA). Immunofluorescence images were obtained with a Zeiss LSM 800 Airyscan microscope using Zeiss ZEN version 2.6 software. Immunofluorescence quantification was completed by using ImageJ software version 1.53k (NIH, Bethesda, MD; *https://imagej.nih.gov/ij*) and calculating for the corrected total cell fluorescence (CTCF) using the following formula: CTCF = integrated density − (area of selected cell × mean fluorescence background readings).

Results

Expression of *Foxi1* was examined in kidneys of heterozygous *Tsc2* ($Tsc2^{+/-}$) mice. Northern blot analyses in Figure 1A show the progression of *Foxi1* expression in kidneys of $Tsc2^{+/-}$ mice. The expression of *Foxi1* in the kidneys of 180- or 300-day–old $Tsc2^{+/-}$ mice was almost comparable to that of WT mice. However, *Foxi1* exhibited a robust induction in the kidneys of 450-day–old $Tsc2^{+/-}$ mice (Figure 1A). The histologic analysis of kidneys by H&E staining showed the absence of any cysts in 180-day–old $Tsc2^{+/-}$ mice, the appearance of a few small cysts at 300 days (Figure 1B), and multiple cysts of varying sizes at 450 days (Figure 1B). Double immunofluorescence labeling with ClC5 and H^+-ATPase antibodies showed a remarkable co-localization of the two molecules on the apical membrane of cyst epithelia in 450-day–old $Tsc2^{+/-}$ mice (Figure 1C). CTCF analysis of $Tsc2^{+/-}$ mice indicates that both ClC5 and H^+-ATPase expression in cystic epithelium exhibit significantly higher fluorescence values compared with background (ClC5, 23,781 ± 3456; background, 3.32 ± 0.08; H^+-ATPase, 20,214 ± 1084; background, 3.52 ± 0.12) (Figure 1C).

Figure 2 explores the proliferation status of kidney cells in the young and old $Tsc2^{+/-}$ mice from Figure 1. Toward this goal, double immunofluorescence labeling with the proliferating cell nuclear antigen (a marker of proliferation) and H^+-ATPase (Figure 2A) or AQP2 (Figure 2B) antibodies was performed. As indicated, there was increased

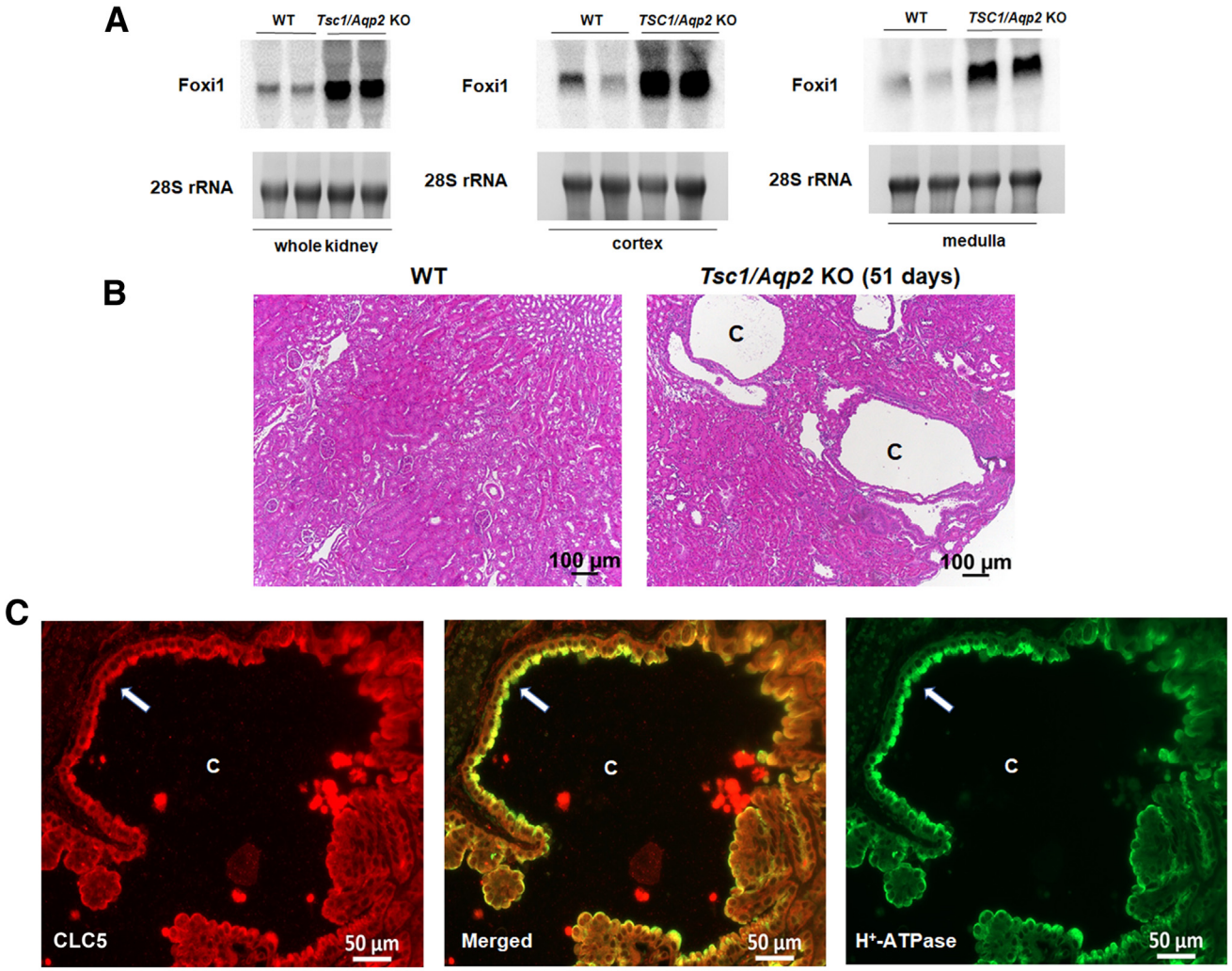

Figure 3 Examination of Foxi1 expression and chloride channel 5 (ClC5) localization in kidneys of wild-type (WT) and *Tsc1* knockout (KO) (*Tsc1/Aqp2* cre) mice. **A:** Expression of *Foxi1* in kidneys of Tsc1 KO mice. Although *Foxi1* is mainly present in the kidney cortex, there is additional up-regulation found in the medulla as well. *Foxi1* expression is low in WT mice. **B:** Histologic analysis of kidneys of WT and *Tsc1* KO mice. Unlike $Tsc2^{+/-}$ mice, which develop cysts at later time points, *Tsc1* KO mice undergo cystogenesis at an earlier age, presenting with large cysts by 51 days of age. Hematoxylin and eosin images are shown. **C:** Double immunofluorescence labeling with ClC5 and H^+-ATPase antibodies in the kidneys of *Tsc1* KO mice. ClC5 (**left panel**) and H^+-ATPase (**right panel**) show striking co-localization in the merged image (**middle panel**). **White arrows** show an example of an area of co-localization between ClC5 and H^+-ATPase. Scale bars: 100 μm (**B**); 50 μm (**C**). Original magnification: ×10 (**B**); ×40 (**C**). "C" represents cysts.

proliferation in cells lining the cysts (day 300), prior to the expansion of cysts in older mice (day 450). Cysts displayed widespread staining for H^+-ATPase expression (Figure 2A), while lacking AQP2 staining in the apical membrane (Figure 2B), consistent with the propagation of A-intercalated cells and the disappearance of principal cells.

FoxI1 plays a critical role in kidney cystogenesis in tuberous sclerosis,[10] as shown by the abrogation of cysts in *Tsc1/Foxi* double-KO mice.[10] As indicated in Figure 3A, *Foxi1* transcript showed a substantial induction in kidneys of *Tsc1/Aqp2* KO mice versus WT mice. Although *Tsc1/Aqp2* KO cyst formation is limited to the kidney cortex, enhanced Foxi1 mRNA expression was detected in both the cortex and medulla (Figure 3A). Histologic analysis of H&E stained samples showed numerous large and small kidney cysts (Figure 3B), and immunofluorescence labeling indicated a robust expression and co-localization of ClC5 and H^+-ATPase on the apical membrane of cyst epithelia in *Tsc1/Aqp2* KO mice (Figure 3C). Image quantification analysis showed that ClC5 (23,816 ± 2420) and H^+-ATPase (35,658 ± 9806) exhibited significantly higher fluorescence values compared with background (ClC5, 5.02 ± 0.83; H^+-ATPase, 2.52 ± 0.49) when analyzed for CTCF (Figure 3C).

Similar to the *Tsc1/Aqp2* KO mice, *Foxi1* expression showed a robust enhancement in kidneys of principal cell–specific *Tsc2* KO mice (Figure 4A). Histologic analysis showed a time-dependent increase in the number and sizes of cysts in kidneys of *Tsc2/Aqp2* KO mice (Figure 4B), with a similar pattern of cyst expansion found in $Tsc2^{+/-}$ aging mice. The double-label immunofluorescence images of ClC5 and H^+-ATPase display remarkable

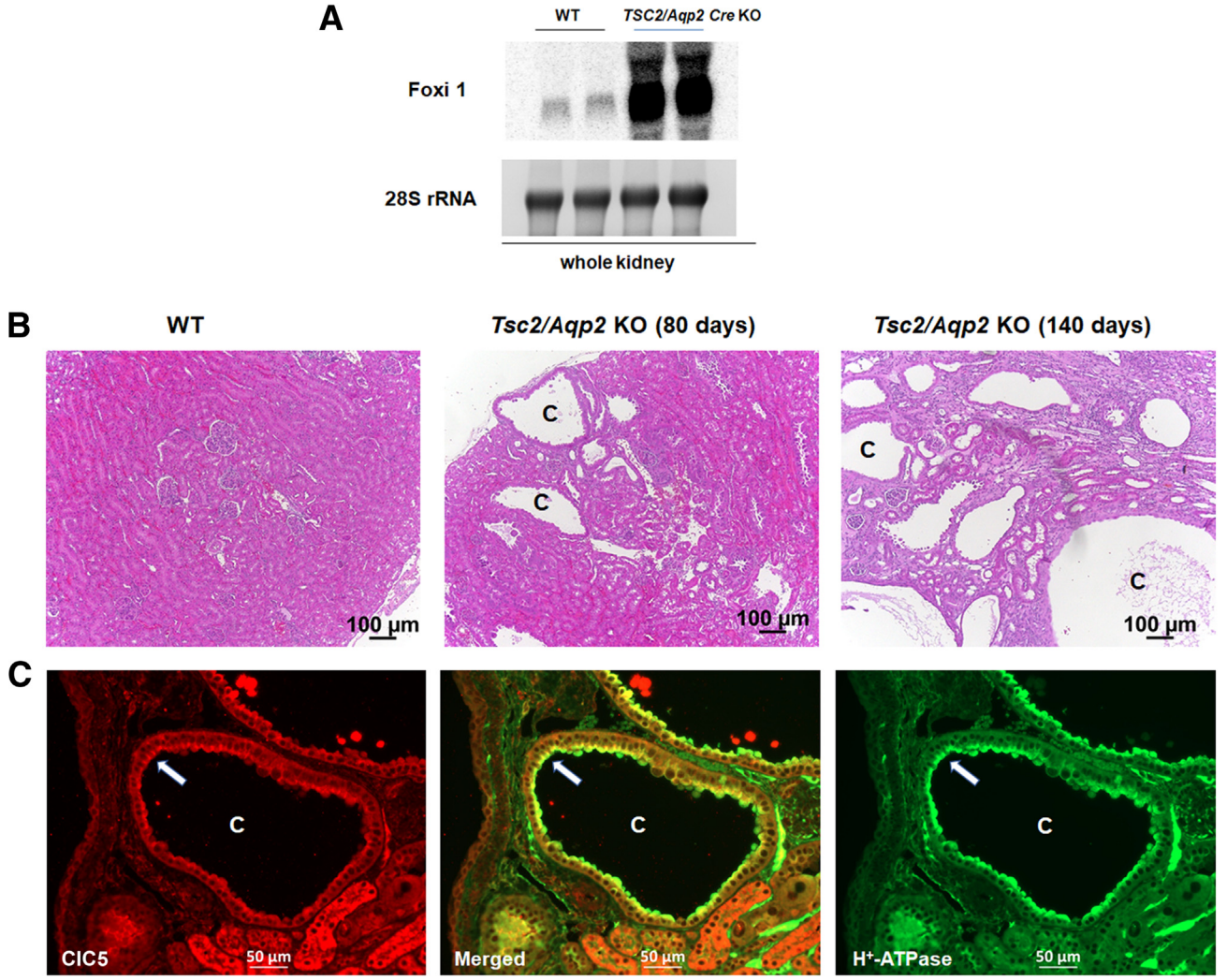

Figure 4 Examination of Foxi1 expression and chloride channel 5 (ClC5) localization in kidneys of wild-type (WT) and *Tsc2* knockout (KO) (*Tsc2/Aqp2* cre) mice. **A:** Expression of *Foxi1* in kidneys of *Tsc2* KO mice. There is a substantial increase in *Foxi1* expression in *Tsc2* KO mice compared with WT mice. **B:** Histologic analysis of kidneys of WT and *Tsc2* KO mice. Hematoxylin and eosin images were obtained from WT and *Tsc2* KO mice at 80 and 140 days of age. Similar to $Tsc2^{+/-}$ mice, there is an age-related cystogenesis that occurs in principal cell–specific *Tsc2* KO mice. **C:** Double immunofluorescence labeling with ClC5 and H^+-ATPase antibodies in kidneys of *Tsc2* KO mice. Images of ClC5 (**right panel**) and H^+-ATPase (**left panel**) in *Tsc2* KO mice are shown. **White arrows** depict areas of co-localizations between the antibodies (merged image; **middle panel**). Scale bars: 100 μm (**B**); 50 μm (**C**). Original magnification: ×10 (**B**); ×40 (**C**). "C" represents cysts.

co-localization of H^+-ATPase and ClC5 along the apical membrane of cystic epithelium in *Tsc2/Aqp2* KO mice (Figure 4C). This is further illustrated by the enhanced immunofluorescence staining (ClC5, 23,816 ± 2421; H^+-ATPase, 25,732 ± 3451) compared with background (ClC5, 2.82 ± 0.96; H^+-ATPase, 5.24 ± 0.22) when analyzed for CTCF.

Expression of *Foxi1* and localization of ClC5 were examined in kidneys of pericyte-specific *Tsc1* KO (*Tsc1/renin* cre) mice. Similar to other models, H&E staining revealed multiple large and small cysts (Supplemental Figure S1A), and double immunofluorescence labeling showed a strong and widespread co-localization of ClC5 and H^+-ATPase on the apical membrane of cyst epithelia in pericyte-specific *Tsc1* KO mice (Supplemental Figure S1B). Further delineation of the importance of the relationship between ClC5 and H^+-ATPase toward cyst formation is observed in human TSC patients (Figure 5A). As indicated, there is a marked apical co-localization of the ClC5 and H^+-ATPase in human kidney cyst epithelium in TSC (Figure 5A).

To determine whether the co-localization of ClC5 and H^+-ATPase in kidney cysts is unique to TSC or is present in other hereditary models of kidney cysts, double immunofluorescence labeling with H^+-ATPase and ClC5 antibodies was performed on cyst epithelium from humans with ADPKD and in kidneys of Pkd1 mice. As shown, ClC5 and H^+-ATPase displayed significantly lower expression versus TSC and exhibited few apical localizations in cyst epithelia in both human ADPKD (Figure 5B) and PKD mice

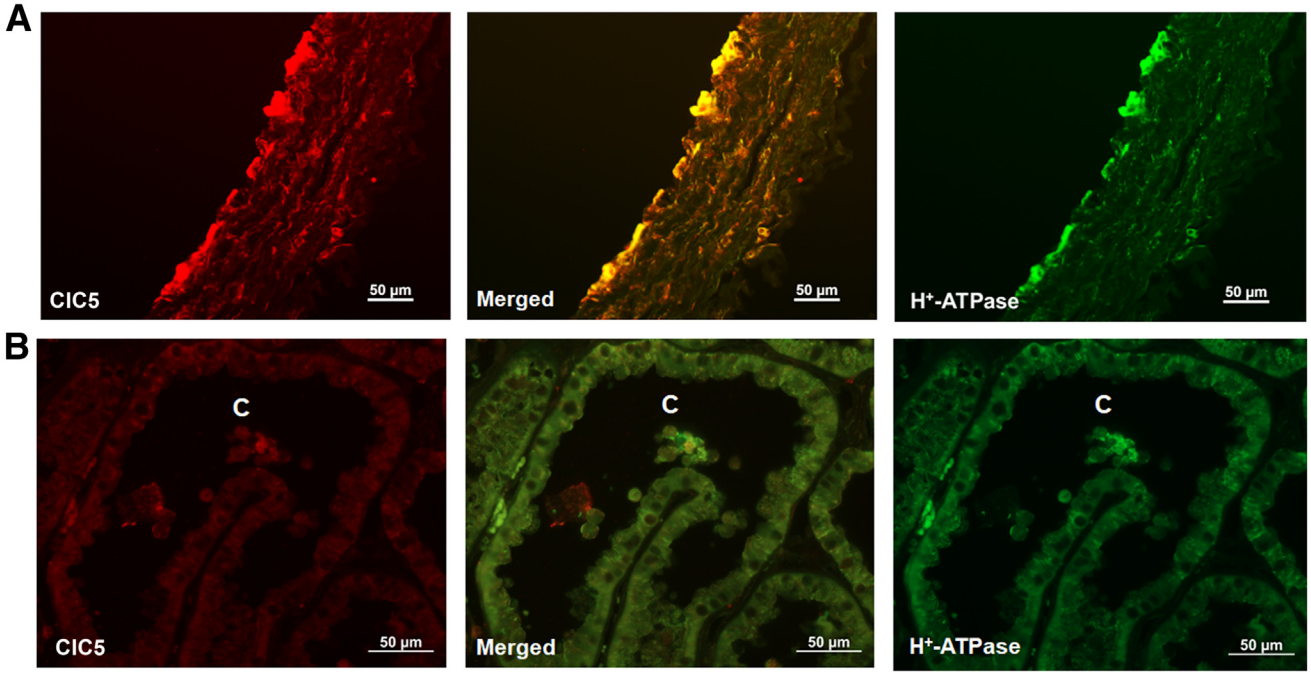

Figure 5 Expression of chloride channel 5 (ClC5) in cystic epithelium from individuals with tuberous sclerosis complex (TSC) or autosomal dominant polycystic kidney disease (ADPKD). **A:** Double immunofluorescence labeling with ClC5 and H^+-ATPase antibodies in an individual with TSC. Similar to TSC mouse models, human cystic epithelium also shows a marked apical co-localization (merged image; **middle panel**) between ClC5 (**right panel**) and H^+-ATPase (**left panel**). **B:** Double immunofluorescence labeling with ClC5 and H^+-ATPase antibodies in an individual with ADPKD. Unlike TSC, humans with ADPKD lack ClC5—positive staining in cyst epithelium. Scale bars = 50 μm. Original magnification, ×40. "C" represents cysts.

(Figure 6A). The double labeling with AQP2 and ClC5 antibodies indicate that the predominant cell type lining the cysts in PKD are principal cells (Figure 6B).

Discussion

The current study shows that ClC5 is strongly expressed on the apical membrane of cyst epithelia in various models of TSC (Figures 1, 2, 3, 4, and 5A). It further indicates that ClC5 is not detected on the apical membrane of cystic epithelia in human or mouse models of PKD (Figures 5B and 6). These data indicate that the specificity of ClC5 localization is unique to TSC kidney cysts where it co-localizes with H^+-ATPase on the apical membrane of cyst epithelia in both TSC patients and various animal models of TSC (Figures 1, 2, 3, 4, and 5A).

ClC5 encodes an electrogenic Cl^-/H^+ exchanger and belongs to the CLC family of Cl^- channels/transporters.[21–23] It is located in the endosomal membrane in proximal tubule and A-intercalated cells of the collecting duct.[21–23] ClC5 plays a critical role in dissipating H^+ secretion and endosomal membrane depolarization mediated via H^+-ATPase by driving Cl^- into the lumen of endosomes in exchange for H^+. The mode of transport of ClC5 is electrogenic and comprises two inward Cl^- ions in exchange for one outward H^+ ion.[21–24] Thus, ClC5 in collaboration with H^+-ATPase allows parallel movement of Cl^- and H^+ into the lumen of endosomes, sustaining a highly acidic environment, which is essential for their physiological function, while preventing the membrane depolarization resulting from the inward transport of H^+ via H^+-ATPase. Inactivating mutations in ClC5 are associated with the development of Dent disease, an X-linked renal tubular disorder characterized by proximal tubule dysfunction, including low-molecular-weight proteinuria, hypercalciuria, nephrocalcinosis, and progressive renal failure.[21–23] There are no pathophysiological processes attributable to ClC5 function in intercalated cells.

The results display the progression of *Foxi1* expression and cyst development in kidneys of $Tsc2^{+/-}$ mice (Figure 1, A and B). As shown in Figure 1A, the expression of *Foxi1* in $Tsc2^{+/-}$ mice remains low and comparable to that in WT mice at 6 and 10 months after birth but shows a robust induction at 15 months of age. Histologic analysis of kidneys in $Tsc2^{+/-}$ mice showed no cysts at 6 months but revealed the appearance of a few small cysts at 10 months of age (Figure 1B). $Tsc2^{+/-}$ kidneys showed numerous large and small cysts at 15 months of age (Figure 1B). The enlargement of cysts in 15-month—old $Tsc2^{+/-}$ mice was associated with a strong and widespread apical expression of ClC5 and H^+-ATPase in cyst epithelium (Figure 1C).

The results in Figure 1 strongly suggest that the initiation of cystogenesis precedes the enhanced expression of *Foxi1* in kidneys of $Tsc2^{+/-}$ mice (300- versus 450-day—old mice). The results in 450-day—old mice show that the robust

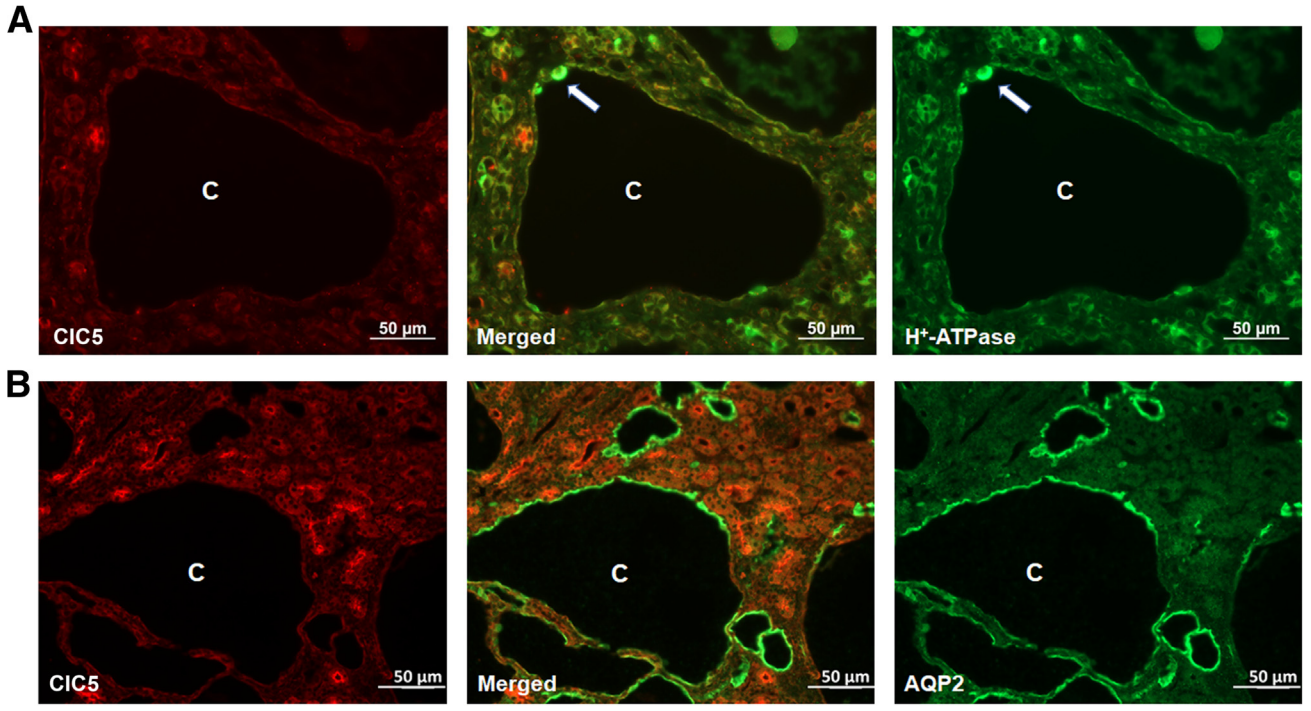

Figure 6 Expression of chloride channel 5 (ClC5) in cystic epithelium of *PKD1* mice. **A:** Double immunofluorescence labeling with ClC5 and H^+-ATPase antibodies in kidneys of *PKD1* mice. Unlike the tuberous sclerosis complex (TSC) mouse models presented in this study, *PKD1* mice express little ClC5—positive staining (**left panel**) in their cystic epithelium. In addition, there are few apical H^+-ATPase—positive cells (**right panel**; **white arrow**) lining the cyst. **Middle panel** shows the merged image. **B:** Double immunofluorescence labeling with ClC5 and AQP2 antibodies in kidneys of *PKD1* mice. There are numerous AQP2-positive cells (**right panel**) lining the cyst; however, no ClC5 staining (**left panel**) is detected. **Middle panel** shows the merged image. Scale bars = 50 μm. Original magnification, ×40. "C" represents cyst.

induction of *Foxi1* was associated with the apical localization of ClC5 and H^+-ATPase in A-intercalated cells lining the cysts (Figure 1C). ClC5 expression in WT mice is limited to the intracellular compartments in proximal tubule and some intercalated cells (Figure 1C). These studies support the notion that the initiation phase of cystogenesis precedes the robust expression of Foxi1. It is likely that enhanced expression of Foxi1 correlates with the expansion of kidney cysts in TSC. The results in Figure 2 indicate that cyst epithelia exhibit robust proliferation in 300-day—old mice, as verified by increased PCNA expression in cyst epithelial cells. These results further support the view that enhanced *Foxi1* expression may be critical to the expansion of cysts and could play a role in the proliferation of cyst epithelia.

Although the expansion of cysts correlates with a significant disappearance of principal cells and proliferation of A-intercalated cells lining the cyst,[19] the exact mechanism for Cl^- transport and, as a consequence, fluid secretion, into the cyst lumen in TSC remains speculative. Unlike principal cells in ADPKD, which secret Cl^- into the cyst lumen via CFTR,[20,36,37] the abundance of CFTR in A-intercalated cells is very low.[38] As such, transporters and/or channels distinct from CFTR may play a critical role in Cl^- secretion into the cyst lumen in TSC.

The initial signal in TSC originates from the inactivating mutations in either the *TSC1* or *TSC2* gene. Functionally, the protein products of these two genes form a complex that is critical to the regulation of cell growth through the phosphatidylinositol 3-kinase signaling pathway, which is a strong inhibitor of the mTOR.[5,39–41] As a result, inactivation in either the *TSC1* or *TSC2* gene results in permanent activation of mTOR complex 1 in various organs.[1–5] Several elegant studies have shown an essential role for H^+-ATPase in amino acid—mediated translocation of mTOR complex 1 to the lysosomal membrane, where it becomes activated.[42–44] H^+-ATPase accomplishes this task by interacting with the Ragulator, a scaffolding complex that anchors the Rag GTPases to the lysosomes and promotes mTOR complex 1 translocation and activation.[37,45,46]

These studies[42–44] show the activation of mTOR1 and H^+-ATPase in lysosomal membrane. However, our studies indicate the activation of mTOR complex 1 and H^+-ATPase in the apical membrane of cell epithelium.[19]

The current studies point to a fundamental difference in mechanisms for Cl^- secretion into the kidney cyst lumen in TSC versus PKD. This difference reflects the distinct cell types lining the cysts in the two kidney cyst models. Although cells lining the cysts in PKD were predominantly composed of principal cells (Figure 6),[36,37] the current studies indicate that the cysts in TSC were overwhelmingly composed of A-intercalated cells. As a result, CFTR, which is the dominant Cl^--secreting molecule in cyst epithelia in PKD, was not a major Cl^--secreting molecule into the cyst

lumen in TSC. The exocytosis of endosomal ClC5 along with H^+-ATPase to the apical membrane of cyst epithelia supports a critical role for an electrogenic $2Cl^-/H^+$ exchanger, ClC5, in mediating Cl^- secretion and cyst expansion in TSC. These are the first reports on the apical membrane localization of ClC5 in A-intercalated cells in any disease state. They suggest that, similar to late endosomes/lysosomes, ClC5 and H^+-ATPase may function synergistically on cyst epithelia by secreting Cl^- and H^+ into the cyst lumen. This coordinated action ensures cyst expansion consequent to Cl^- secretion. Maneuvers aimed at inhibiting ClC5 may have therapeutic effects in decreasing cyst burden in TSC.

Author Contributions

S.B. performed experiments, generated figures, and edited the manuscript; M.B. performed experiments; K.Z. performed experiments and edited the manuscript; L.S.H. provided reagents; J.B. and J.J.Y. provided animal models; and M.S. conceptualized the experiments, interpreted the results, and wrote the manuscript.

Supplemental Data

Supplemental material for this article can be found at *http://doi.org/10.1016/j.ajpath.2022.10.007*.

References

1. Sampson JR, Harris PC: The molecular genetics of tuberous sclerosis. Hum Mol Genet 1994, 3:1477–1480
2. Henske EP, Józwiak S, Kingswood JC, Sampson JR, Thiele EA: Tuberous sclerosis complex. Nat Rev Dis Primers 2016, 2:16035
3. Dixon BP, Hulbert JC, Bissler JJ: Tuberous sclerosis complex renal disease. Nephron Exp Nephrol 2011, 118:e15–e20
4. Crino PB, Nathanson KL, Henske EP: The tuberous sclerosis complex. N Engl J Med 2006, 355:1345–1356
5. Henske EP, Rasooly R, Siroky B, Bissler J: Tuberous sclerosis complex, mTOR, and the kidney: report of an NIDDK-sponsored workshop. Am J Physiol Renal Physiol 2014, 306:F279–F283
6. Bissler JJ, McCormack FX, Young LR, Elwing JM, Chuck G, Leonard JM, Schmithorst VJ, Laor T, Brody AS, Bean J, Salisbury S, Franz DN: Sirolimus for angiomyolipoma in tuberous sclerosis complex or lymphangioleiomyomatosis. N Engl J Med 2008, 358: 140–151
7. Long X, Ortiz-Vega S, Lin Y, Avruch J: Rheb binding to mammalian target of rapamycin (mTOR) is regulated by amino acid sufficiency. J Biol Chem 2005, 280:23433–23436
8. Inoki K, Li Y, Xu T, Guan K-L: Rheb GTPase is a direct target of TSC2 GAP activity and regulates mTOR signaling. Genes Dev 2003, 17:1829–1834
9. Bissler JJ, Kingswood JC, Radzikowska E, Zonnenberg BA, Frost M, Belousova E, Sauter M, Nonomura N, Brakemeier S, de Vries PJ, Whittemore VH, Chen D, Sahmoud T, Shah G, Lincy J, Lebwohl D, Budde K: Everolimus for angiomyolipoma associated with tuberous sclerosis complex or sporadic lymphangioleiomyomatosis (EXIST-2): a multicentre, randomised, double-blind, placebo-controlled trial. Lancet 2013, 381:817–824
10. Tarasewicz A, Debska-Slizień A, Konopa J, Zdrojewski Z, Rutkowski B: Rapamycin as a therapy of choice after renal transplantation in a patient with tuberous sclerosis complex. Transplant Proc 2009, 41:3677–3682
11. Rosset C, Netto CBO, Ashton-Prolla P: TSC1 and TSC2 gene mutations and their implications for treatment in tuberous sclerosis complex: a review. Genet Mol Biol 2017, 40:69–79
12. De Waele L, Lagae L, Mekahli D: Tuberous sclerosis complex: the past and the future. Pediatr Nephrol 2015, 30:1771–1780
13. Palavra F, Robalo C, Reis F: Recent advances and challenges of mTOR inhibitors use in the treatment of patients with tuberous sclerosis complex. Oxid Med Cell Longev 2017, 2017:9820181
14. Bissler JJ, Kingswood JC: Optimal treatment of tuberous sclerosis complex associated renal angiomyolipomata: a systematic review. Ther Adv Urol 2016, 8:279–290
15. Onda H, Lueck A, Marks PW, Warren HB, Kwiatkowski DJ: Tsc2(+/-) mice develop tumors in multiple sites that express gelsolin and are influenced by genetic background. J Clin Invest 1999, 104:687–695
16. Bonsib SM, Boils C, Gokden N, Grignon D, Gu X, Higgins JPT, Leroy X, McKenney JK, Nasr SH, Phillips C, Sangoi AR, Wilson J, Zhang PL: Tuberous sclerosis complex: hamartin and tuberin expression in renal cysts and its discordant expression in renal neoplasms. Pathol Res Pract 2016, 212:972–979
17. Lam HC, Nijmeh J, Henske EP: New developments in the genetics and pathogenesis of tumours in tuberous sclerosis complex. J Pathol 2017, 241:219–225
18. Bissler JJ, Zadjali F, Bridges D, Astrinidis A, Barone S, Yao Y, Redd JR, Siroky BJ, Wang Y, Finley JT, Rusiniak ME, Baumann H, Zahedi K, Gross KW, Soleimani M: Tuberous sclerosis complex exhibits a new renal cystogenic mechanism. Physiol Rep 2019, 7:e13983
19. Barone S, Zahedi K, Brooks M, Henske EP, Yang Y, Zhang E, Bissler JJ, Yu JJ, Soleimani M: Kidney intercalated cells and the transcription factor FOXi1 drive cystogenesis in tuberous sclerosis complex. Proc Natl Acad Sci U S A 2021, 118. e2020190118
20. Edwards ME, Chebib FT, Irazabal MV, Ofstie TG, Bungum LA, Metzger AJ, Senum SR, Hogan MC, El-Zoghby ZM, Kline TL, Harris PC, Czerwiec FS, Torres VE: Long-term administration of tolvaptan in autosomal dominant polycystic kidney disease. Clin J Am Soc Nephrol 2018, 13:1153–1161
21. Piwon N, Günther W, Schwake M, Bösl MR, Jentsch TJ: ClC-5 Cl^--channel disruption impairs endocytosis in a mouse model for Dent's disease. Nature 2000, 408:369–373
22. Devuyst O, Christie PT, Courtoy PJ, Beauwens R, Thakker RV: Intra-renal and subcellular distribution of the human chloride channel, CLC-5, reveals a pathophysiological basis for Dent's disease. Hum Mol Genet 1999, 8:247–257
23. Günther W, Lüchow A, Cluzeaud F, Vandewalle A, Jentsch TJ: ClC-5, the chloride channel mutated in Dent's disease, colocalizes with the proton pump in endocytotically active kidney cells. Proc Natl Acad Sci U S A 1998, 95:8075–8080
24. Satoh N, Suzuki M, Nakamura M, Suzuki A, Horita S, Seki G, Moriya K: Functional coupling of V-ATPase and CLC-5. World J Nephrol 2017, 6:14–20
25. Blomqvist SR, Vidarsson H, Fitzgerald S, Johansson BR, Ollerstam A, Brown R, Persson AEG, Bergström GG, Enerbäck S: Distal renal tubular acidosis in mice that lack the forkhead transcription factor Foxi1. J Clin Invest 2004, 113:1560–1570
26. Vidarsson H, Westergren R, Heglind M, Blomqvist SR, Breton S, Enerbäck S: The forkhead transcription factor Foxi1 is a master regulator of vacuolar H-ATPase proton pump subunits in the inner ear, kidney and epididymis. PLoS One 2009, 4:e4471
27. Kwiatkowski DJ, Zhang H, Banduar JL, Heiberger KM, Glogauer M, el-Hashemite N, Onda H: A mouse model of TSC1 reveals sex-dependent lethality from liver hemangiomas, and up-regulation of p70S6 activity in Tsc1 null cells. Hum Mol Genet 2002, 11:525–534
28. Meikle L, McCullen JR, Sherwood MC, Lader AS, Walker V, Chan JA, Kwiatkowski DJ: A mouse model of cardiac rhabdomyoma

generated by loss of Tsc1 in ventricular myocytes. Hum Mol Genet 2005, 14:429–435
29. Hernandez O, Way S, McKenna J 3rd, Gambello MJ: Generation of a conditional disruption of the Tsc2 gene. Genesis 2007, 45:101–106
30. Nelson RD, Stricklett P, Gustafson C, Stevens A, Ausiello D, Brown D, Kohan DE: Expression of an AQP2 Cre recombinase transgene in kidney and male reproductive system of transgenic mice. Am J Physiol 1998, 275:C216–C226
31. Stricklett PK, Nelson RD, Kohan DE: Targeting collecting tubules using the aquaporin-2 promoter. Exp Nephrol 1999, 7:67–74
32. Glenn ST, Jones CA, Pan L, Gross KW: In vivo analysis of key elements within the renin regulatory region. Physiol Genomics 2008, 35:243–253
33. Xu J, Worrell RT, Li HC, Barone SL, Petrovic S, Amlal H, Soleimani M: Chloride/bicarbonate exchanger SLC26A7 is localized in endosomes in medullary collecting duct cells and is targeted to the basolateral membrane in hypertonicity and potassium depletion. J Am Soc Nephrol 2006, 17:956–967
34. Xu J, Barone S, Li H, Holiday S, Zahedi K, Soleimani M: Slc26a11, a chloride transporter, localizes with the vacuolar H^+-ATPase of A-intercalated cells of the kidney. Kidney Int 2011, 80:926–937
35. Barone S, Xu J, Zahedi K, Brooks M, Soleimani M: Probenecid pretreatment downregulates the kidney $Cl^-/HCO3^-$ exchanger (pendrin) and potentiates hydrochlorothiazide-induced diuresis. Front Physiol 2018, 9:849
36. Shibazaki S, Yu Z, Nishio S, Tian X, Thomson RB, Mitobe M, Louvi A, Velazquez H, Ishibe S, Cantley LG, Igarashi P, Somlo S: Cyst formation and activation of the extracellular regulated kinase pathway after kidney specific inactivation of Pkd1. Hum Mol Genet 2008, 17:1505–1516
37. Holthöfer H, Kumpulainen T, Rapola J: Polycystic disease of the kidney. Evaluation and classification based on nephron segment and cell-type specific markers. Lab Invest 1990, 62:363–369
38. Kia MV, Barone S, McDonough AA, Zahedi K, Xu J, Soleimani M: Downregulation of the $Cl^-/HCO3^-$ exchanger pendrin in kidneys of mice with cystic fibrosis: role in the pathogenesis of metabolic alkalosis. Cell Physiol Biochem 2018, 45:1551–1565
39. Yang Q, Guan KL: Expanding mTOR signaling. Cell Res 2007, 17:666–681
40. Brugarolas J, Lei K, Hurley RL, Manning BD, Reiling JH, Hafen E, Witters LA, Ellisen LW, Kaelin WG Jr: Regulation of mTOR function in response to hypoxia by REDD1and the TSC1/TSC2 tumor suppressor complex. Genes Dev 2004, 18:2893–2904
41. Fingar DC, Salama S, Tsou C, Harlow E, Blenis J: Mammalian cell size is controlled by mTOR and its downstream targets S6K1 and 4EBP1/eIF4E. Genes Dev 2002, 16:1472–1487
42. Yan Y, Denef N, Schüpbach T: The vacuolar proton pump, V-ATPase, is required for Notch signaling and endosomal trafficking in Drosophila. Dev Cell 2009, 17:387–402
43. Peña-Llopis S, Vega-Rubin-de-Celis S, Schwartz JC, Wolff NC, Tran TAT, Zou L, Xie X-J, Corey DR, Brugarolas J: Regulation of TFEB and V-ATPases by mTORC1. EMBO J 2011, 30:3242–3258
44. Zoncu R, Bar-Peled L, Efeyan A, Wang S, Sancak Y, Sbatini DM: mTORC1 senses lysosomal amino acids through an inside-out mechanism that requires the vacuolar H(+)-ATPase. Science 2011, 334:678–683
45. Zhang M-Z: Notch signaling is essential in collecting duct epithelial cell fate determination during development and maintenance of cell type homeostasis in adult. Ann Transl Med 2019, 7(Suppl 8):S376
46. Murthy V, Haddad LA, Smith N, Pinney D, Tyszkowski R, Brown D, Ramesh V: Similarities and differences in the subcellular localization of hamartin and tuberin in the kidney. Am J Physiol Renal Physiol 2000, 278:F737–F746